

Gas-Liquid Interfacial Area, Bubble Size and Liquid-Phase Mass Transfer Coefficient in a Three-Phase External Loop Airlift Bubble Column

M. Yoshimoto, S. Suenaga, K. Furumoto*, K. Fukunaga, and Katsumi Nakao[†]

Department of Applied Chemistry and Chemical Engineering,
Yamaguchi University, Tokiwadai, Ube, Yamaguchi 755-8611, Japan
e-mail: knakao@yamaguchi-u.ac.jp

*Oshima National College of Maritime Technology, Oshima,
Yamaguchi 742-2106, Japan

Original scientific paper
Received: May 29, 2007
Accepted: October 15, 2007

The interfacial area a was measured by the sulfite oxidation method in a three-phase external loop airlift bubble column suspending completely the different concentrations of ion exchange resin particles in aqueous carboxymethyl cellulose (CMC) solutions with a wide range of viscosity. The column had been previously studied for the circulating liquid velocity U_L , gas holdup ε_G and volumetric gas-liquid oxygen transfer coefficient $k_L a$ in the two- and three-phase systems. The average bubble size d_B and oxygen transfer coefficient k_L were obtained as $d_B = 6 \varepsilon_G / a$ and $k_L = (\text{the previous } k_L a) / a$, respectively. The similar studies were carried out in the internal loop airlift and normal bubble columns for comparison. The a values in the external loop airlift were found to be little affected by the column height and particles concentrations, and to decrease with increasing viscosity. All the three columns showed a linear dependence of a on ε_G . A simple correlation of a , d_B or k_L was proposed as a function of ε_G and viscosity for the external loop airlift as well as both internal loop airlift and normal columns. A well-known relationship between k_L and d_B was confirmed to hold independent of column types and operating conditions for a given two or three phase system.

Key words:

External loop airlift, three phase flow, suspended solid particles, interfacial area, bubble size, oxygen transfer coefficient

Introduction

Much work has been done on the hydrodynamics and mass transfer in the gas-liquid two phase flow in the external loop airlift bubble column (ELBC).¹⁻⁴ The unique feature of ELBC is its more well-defined recirculating liquid flow pattern which makes the hydrodynamic and mass transfer properties different from those in the internal loop airlift bubble column (ILBC) and normal bubble column (NBC). Especially, the liquid circulation makes it easier for the solid particles charged to be completely and uniformly suspended in ELBC than in either ILBC or NBC. Recently, more attention has been paid to the hydrodynamics and mass transfer in the gas-liquid-solid three phase flow in ELBC.⁵⁻⁷ The effects of suspended solid particles on the gas holdup ε_G and volumetric gas-liquid mass transfer coefficient $k_L a$ have extensively been studied in the three phase ELBC.^{8,9} Although there have been a few studies on the gas-liquid interfacial area a in the two phase ELBC,^{3,4} however, little work has been carried out on a in the three phase ELBC. The data on a provide the results on the average bubble

diameter d_B and gas-liquid mass transfer coefficient k_L calculated as $d_B = 6\varepsilon_G/a$ and $k_L = k_L a/a$, respectively. These informations suggest the behavior of bubbles such as the bubble coalescence and breakup which are governed by the system and operating variables as well as the bubble column designs, and are used to determine the column characteristics including ε_G , $k_L a$, a etc.

The purpose of this work is to (a) measure a by the sulfite oxidation method in the two- and three-phase flows in ELBC as well as both ILBC and NBC, (b) determine d_B from the a and ε_G values observed simultaneously and k_L from dividing by a the $k_L a$ values observed in tap water with and without carboxymethyl cellulose (CMC) separately, (c) examine the effects on the a , d_B and k_L values of the suspended solid particles, liquid viscosity, superficial gas velocity and bubble column design, and (d) correlate the data on a , d_B and k_L with ε_G and the peculiar liquid viscosity μ_p easily measured by the Ostwald-type viscometer based on our previous correlations of ε_G and $k_L a$ for the two phase flow.²

[†]Corresponding author

Experimental

The apparatus used were almost the same as those in our previous work on the gas-liquid two phase flows.² Fig. 1(a) shows a schematic diagram of the external loop airlift bubble column (ELBC). As shown in Fig. 1(b), the internal loop airlift bubble column (ILBC) had a draft tube of 5 cm in diameter with gas injection into the annular section of the ILBC. The 9.5 mm porcelain Raschig rings were packed beneath the perforated plate. The ILBC was used as the normal bubble column (NBC) by removing the draft tube. Table 1 summarizes the experimental conditions.

The values of $k_L a$ were previously obtained by carrying out both the desorption of dissolved oxygen into nitrogen gas flow and the absorption of oxygen in air flow into the aqueous phase in the three phase column.¹⁰ The time course of the dissolved oxygen electrode inserted in the liquid phase through the column wall as shown in Fig. 1(a). The liquids used were tap water and aqueous 0.5 to 2.0 % carboxymethyl cellulose (CMC) solutions. CMC was used to increase the liquid viscosity.

The gas holdup ε_G in the gas-liquid-solid three phase flow in the riser of the ELBC was determined from an analysis of the gradient of static pressure along the column height considering the pressure due to suspended solid particles. The ε_G values in the ILBC and NBC were measured by the volume expansion method.

The circulating superficial liquid velocity U_L in the three phase flow through the riser was measured in the same way as in the two phase flow in our previous work^{2,10} using a plastic sphere of 1.2 cm diameter having the same density as the liquid

Table 1 – Experimental conditions for specific interfacial area

Gas: Air, Superficial gas velocity $U_G = 0.02 \sim 0.32$ m/s
Liquid: Aqueous sodium sulphite solution
0.5 kmol/m ³ Na ₂ SO ₃ /, 0.8, 1.2 wt% CMC/Tap water
Cobalt catalyst conc. $C_{CoSO_4} = 5 \times 10^{-4}$ kmol/m ³ , pH = 8.5
Static liquid height $H_T = 1 \sim 4$ m (ELBC), 0.8 m (ILBC, NBC)
Solid: Ion exchange resin (IR) ($d_p = 450 \mu\text{m}$, $\rho_s = 1252$ kg/m ³)
Solid concentration $C_s = 0 \sim 0.10$ kg/dm ³ -slurry
Temp.: 298~300K

phase in the downcomer almost free of gas bubbles. The velocity in the downcomer was multiplied by the ratio of downcomer cross sectional area A_d to riser one A_r to obtain the U_L value.

The rheological properties of the CMC solutions without salts for the previous determination of $k_L a$ were measured at 298 K with a concentric cylinder viscometer. The values of both the fluid consistency index K and the flow behavior index n were reported in our previous paper.² For convenience, the peculiar viscosity μ_p was also measured using a Ostwald-type viscometer. The a value were measured at room temperature (293 to 300 K) in the case of water without CMC. The temperature of the solution with CMC in the taller ELBC was kept at almost constant of 298 K by a temperature controller unit installed in the gas-liquid separator since a higher liquid viscosity was more sensitive to a change in temperature.

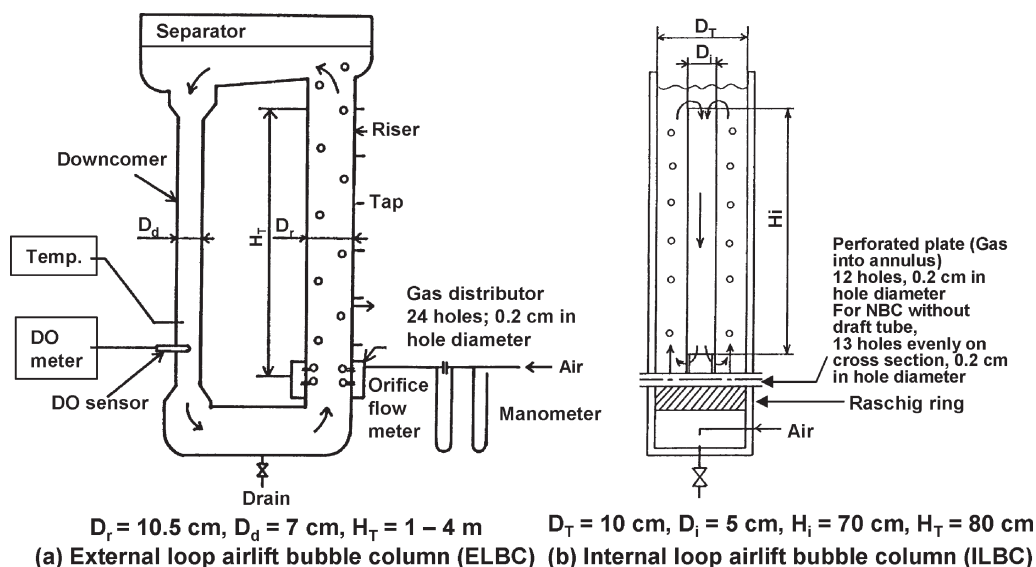


Fig. 1 – Experimental apparatus. (a) External loop airlift bubble column (ELBC), (b) Internal loop airlift bubble column (ILBC)

The liquid used for measurement of a was tap water containing 0.5 kmol/m^3 sodium sulfite Na_2SO_3 and $5 \cdot 10^{-4} \text{ kmol/m}^3$ cobalt sulfate CoSO_4 as a catalyst for the sulfite oxidation by air. The chemical oxygen absorption rate R_{O_2} [$\text{kmol/m}^3\text{s}$] based on the liquid volume was obtained as one half of the rate of decrease in the sulfite concentration which was determined by iodometric titration. CMC was added to the sulfite solution to vary the liquid viscosity. The viscosity was measured by the same Ostwalde-type viscometer as described above. The ion exchange resin (IR) particles of $450 \mu\text{m}$ in mean diameter were used to examine an effect of suspended solid particles on a .

Measurement of gas-liquid interfacial area a

According to the previous kinetic studies on the oxidation of Na_2SO_3 by air based on the chemical absorption theory,¹¹ the absorption rate R_{O_2} is expressed by the following equation, which holds for the pseudo first order regime in the theory.

$$R_{\text{O}_2} = \{a/(1-\varepsilon_G-\varepsilon_S)\} \{(2/3)k_2D_{\text{O}_2}\}^{1/2}C_{\text{O}_i}^{3/2} \quad (1)$$

Where a is the interfacial area based on the dispersion volume, $\varepsilon_S = (1-\varepsilon_G)C_S/\rho_S$ the solid holdup, k_2 [$\text{m}^3/\text{kmol} \cdot \text{s}$] the rate constant for the reaction of the second and zero-th order with respect to the dissolved oxygen and sulfite concentration, respectively, D_{O_2} [m^2/s] the liquid diffusivity of oxygen and C_{O_i} [kmol/m^3] the dissolved oxygen concentration at the gas-liquid interface calculated from the oxygen partial pressure in the gas phase P_{O_2} [Pa] and Henry's law constant H [$\text{kmol/Pa} \cdot \text{m}^3$] as $C_{\text{O}_i} = H P_{\text{O}_2}$.

From the analysis on the kinetic data on the sulfite oxidation by air carried out in the stirred cell with a known flat gas-liquid interface, i.e., a known value of a in Eq. (1), k_2 was determined under the condition of $C_{\text{Na}_2\text{SO}_3} = 0.5 \text{ kmol/m}^3$, $\text{pH} = 8.5$ and $T = 288\text{--}308 \text{ K}$ as follows.

$$k_2 = 2.36 \times 10^{19} C_{\text{CaSO}_4} \exp(-5.13 \times 10^7/RT) \quad (2)$$

where $R = 8.314 \text{ Pa} \cdot \text{m}^3/\text{kmol} \cdot \text{K}$ is the gas constant and C_{CoSO_4} [kmol/m^3] is the CoSO_4 catalyst concentration. Addition of CMC to the solution exerted no effect on the k_2 value. The chemical absorption theory with the result of Eq. (2) verifies that the above conditions of $0.5 \text{ kmol/m}^3 \text{ Na}_2\text{SO}_3$, $5 \times 10^{-4} \text{ kmol/m}^3 \text{ CoSO}_4$, $\text{pH} = 8.5$ and $T = 293\text{--}300 \text{ K}$ satisfy the requirements for the pseudo first order regime, i.e., Eq. (1). Therefore, the a values in any type of bubble columns can be obtained from the following Eq. (1a) by measuring the R_{O_2} values.

$$a = R_{\text{O}_2}(1 - \varepsilon_G - \varepsilon_S)/[\{(2/3)k_2D_{\text{O}_2}\}^{1/2}C_{\text{O}_i}^{3/2}] \quad (1a)$$

In the case of ELBC, the R_{O_2} value above should be obtained by noting that the observed sulfite concentrations were always diluted due to the downcomer under the assumption of the well mixed flow in the whole column. Thus, the apparent value of R_{O_2} , $R_{\text{O}_2}^{\text{app}}$, was converted to the R_{O_2} value in the riser in the following way.

$$R_{\text{O}_2} = R_{\text{O}_2}^{\text{app}}(V_L/V_{\text{Lr}}) \quad (3)$$

where V_L and V_{Lr} are the total and riser liquid volumes, respectively. Assuming the gas phase in plug flow in any type of columns, the C_{O_i} value in Eq. (1a) was determined as the value in equilibrium with the average oxygen partial pressure \bar{P}_{O_2} , i.e., $C_{\text{O}_i} = H\bar{P}_{\text{O}_2}$. The \bar{P}_{O_2} value was calculated as the logarithmic mean of the inlet and outlet oxygen partial pressures. The latter pressure was determined from the oxygen balance with the R_{O_2} value above.

The average bubble diameter d_B was calculated from the observed values of ε_G and a as follows.

$$d_B = 6\varepsilon_G/a \quad (4)$$

The liquid phase oxygen transfer coefficient k_L was calculated from dividing by the observed a value the corresponding $k_L a$ value for the two phase having the same liquid viscosity as the three phase concerned.

$$k_L = k_L a/a \quad (5)$$

The determination was based on the facts that the $k_L a$ values in the three phase ELBC were reproduced by the $k_L a$ correlation for the two phase ELBC¹⁰ and that even in the case of NBC, of which characteristics are known to be more sensitive to the liquid properties compared to ELBC, the $k_L a$ values determined in the CMC solution containing sodium sulfate followed their $k_L a$ correlation proposed for pure CMC solution.¹² Analogously, the d_B and k_L values for both ILBC and NBC were calcu-

Table 2 - Correlations for U_L , ε_G and $k_L a$ in gas-liquid system using μ_P^2

ELBC	$U_L = 1.80 (A_d/A_r)^{0.75} U_G^{0.40} \mu_P^{-0.028} H_T^{0.31}$	$(\mu_P \leq 0.04 \text{ Pa} \cdot \text{s})$ (6a)
	$U_L = 0.67 (A_d/A_r)^{0.75} U_G^{0.40} \mu_P^{-0.33} H_T^{0.31}$	$(\mu_P > 0.04 \text{ Pa} \cdot \text{s})$ (6b)
ELBC	$U_G/\varepsilon_G = \{0.49 + 2.25 (U_G + U_L)\} \mu_P^{0.103}$	(7)
ILBC, NBC	$U_G/\varepsilon_G = 0.49 \mu_P^{0.103} + 2.4 U_G$	(8)
ELBC	$k_L a = 6.60 \times 10^{-2} \varepsilon_G^{1.2} \mu_P^{-0.36}$	(9)
ILBC, NBC	$k_L a = 3.35 \times 10^{-2} \varepsilon_G^{1.1} \mu_P^{-0.33}$	(10)

lated. Table 2 shows our previous correlations of $k_L a$ for the two phase flow ELBC, ILBC and NBC using the peculiar liquid viscosity μ_p for convenience.² The table also includes the correlations of U_L in ELBC and the correlations of ε_G in three types of columns.

Results and discussion

Effect of static liquid height H_T on interfacial area a and gas holdup ε_G in ELBC

Fig. 2(a) and 2(b) show respectively the a and ε_G values in ELBC using aqueous 0.5 kmol/m³ Na₂SO₃ solution as a function of the superficial gas velocity U_G with H_T as a parameter. The a values are seen to be almost unaffected by H_T and to show almost the same variation with U_G in the range of U_G less than 0.1 m/s as those reported by Popovic & Robinson (1987a)³, while the ε_G values to be a little affected by H_T as represented by the previous correlation Eq. (7) shown in Table 2. The former result may be due the fact that the bubble coalescence was retarded by the higher upward liquid velocity with the higher H_T as well as the presence of a coalescence-inhibiting electrolyte Na₂SO₃. The variation of a with U_G are found to be parallel to that of ε_G . The circulating liquid superficial velocity U_L in

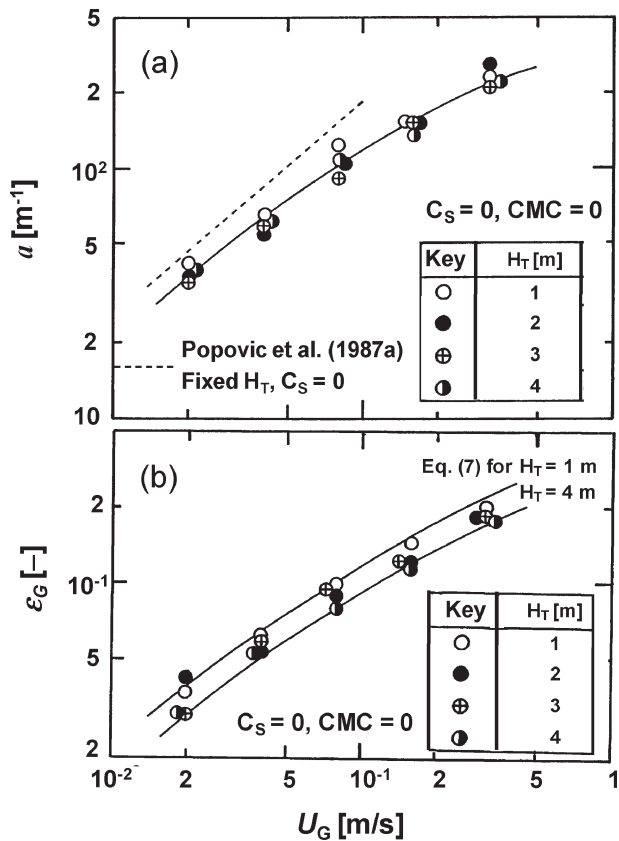


Fig. 2 - Effect of H_T on (a) a and (b) ε_G as a function of U_G (ELBC)

the riser was also observed to agree well with the previous U_L correlation Eq. (6a).

Effect of liquid viscosity on a and ε_G

Fig. 3(a) and 3(b) show the variations of the a and ε_G values with U_G , respectively, in three types of bubble columns with the liquid viscosity as a parameter. It is seen in the figures that the variation of a with U_G is parallel to that of ε_G at any viscosity in any type of columns, that a decreases with increasing viscosity in any column while ε_G is little affected by the viscosity, and that the a values in three columns have almost the same value at a fixed liquid viscosity although the ε_G values in the ILBC and NBC are larger than the those in the ELBC. These results on a arise from an enhancement of bubble coalescence due to increased viscosity in any column and a more retardation of bubble coalescence in the ELBC than in ILBC and NBC due to a higher upward liquid velocity in the riser. On

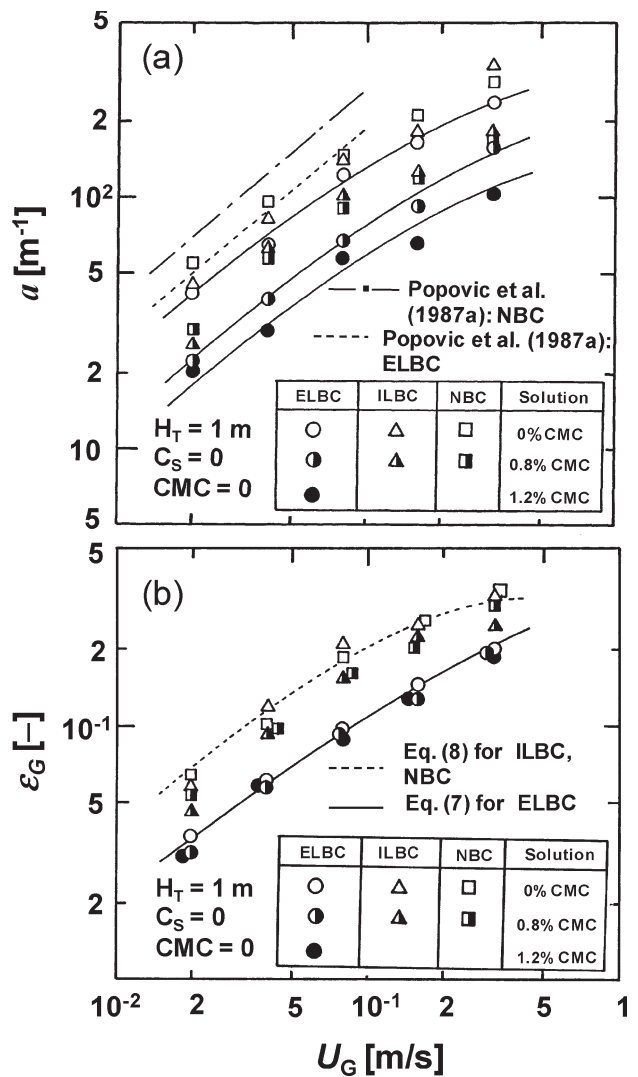


Fig. 3 - Effect of liquid viscosity on (a) a and (b) ε_G as a function of U_G

the other hand, the liquid velocity causes the lower ϵ_G value in the ELBC compared to that in either ILBC or NBC. The ϵ_G values observed in the ELBC as well as the ILBC and NBC are found to agree with those calculated respectively by Eq. (7) and Eq. (8) in Table 2.

Effect of solid particles concentration C_S on a and ϵ_G

Fig. 4(a) and 4(b) represent the change of the a and ϵ_G values with U_G , respectively, in the three bubble columns with C_S as a parameter. Fig. 4(a) suggests that the suspended solid particles increase the a value a little under a certain condition. This may be due to an enhancement of bubble breakup by suspended solid particles. Because of no clear tendency and a small effect exerted by the particles, the effect of particles on a is considered to be neglected in the sulfite solution. No effect of particles on ϵ_G in any column is more clearly shown in Fig. 4(b). The ϵ_G values are also seen to be reproduced by Eqs. (7) and (8) in Table 2.

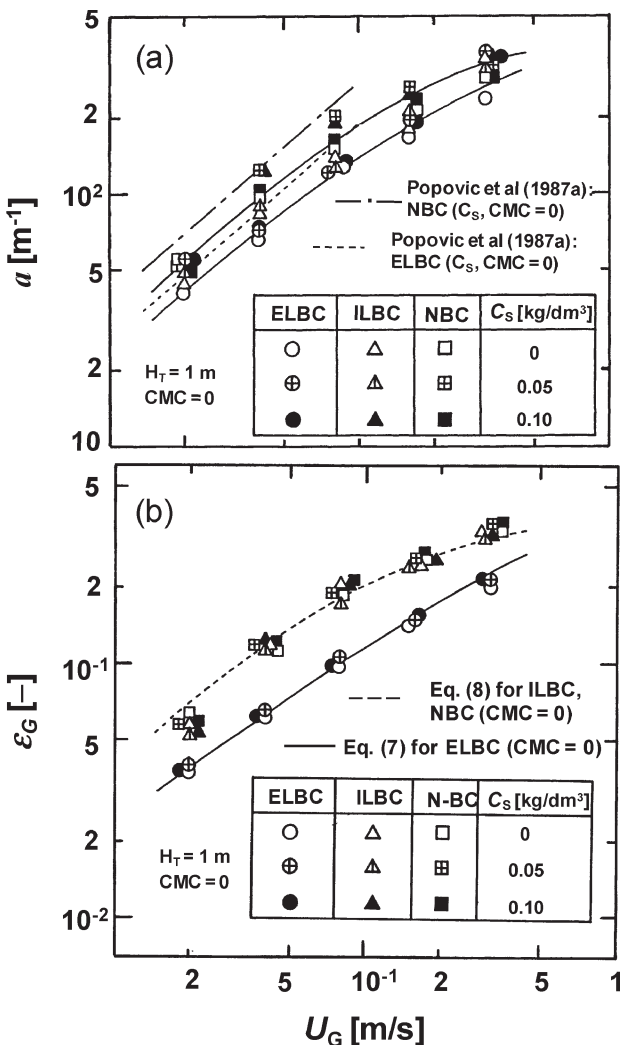


Fig. 4 - Effect of C_S on (a) a and (b) ϵ_G as a function of U_G

Dependence of d_B on H_T , liquid viscosity and C_S

Fig. 5(a), 5(b) and 5(c) show the d_B values calculated by Eq. (4) as a function of U_G with the parameters of the H_T in ELBC and the liquid viscosity and C_S in three columns, respectively. It is seen in the figures that the d_B values are approximately independent of U_G in any values of H_T , liquid viscosity and C_S , that at a fixed value of U_G , H_T exerts no effect on d_B in ELBC, that in any type of column, C_S slightly influences d_B although no clear tendency is found and hence is regarded to unaffected d_B , and that increasing the liquid viscosity clearly increases d_B

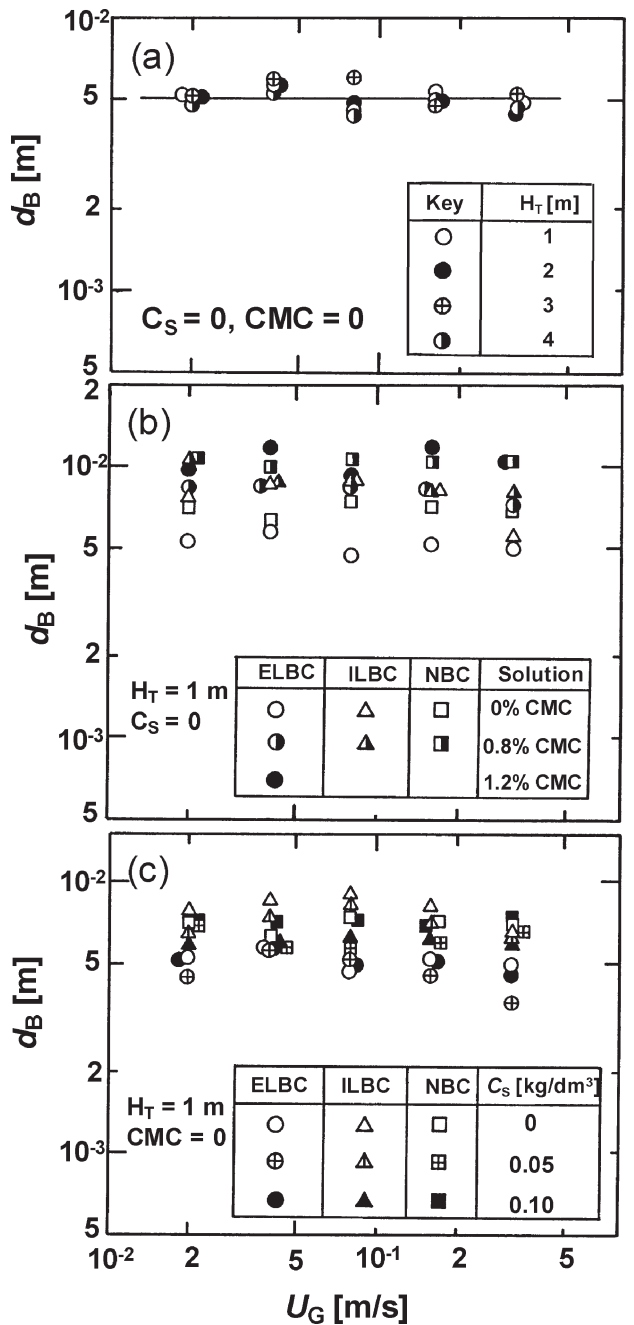


Fig. 5 - Effects of (a) H_T , (b) liquid viscosity and (c) C_S on d_B as a function of U_G

due to an enhanced bubble coalescence in the more viscous solution. A complicated small variation of d_B with U_G at any values of H_T , liquid viscosity and C_S suggests an interaction among these variables governing a balance between the bubble coalescence and breakup frequencies. It is also noted that the d_B value in the ELBC is lower than that in either ILBC or NBC under the same conditions of U_G , viscosity and C_S because of a retarded bubble coalescence caused by a high upward liquid velocity in the riser of ELBC. The d_B values in the ILBC are found to be approximated by those in the NBC.

Dependence of k_L on H_T , liquid viscosity and C_S

Fig. 6(a), 6(b) and 6(c) represent the variations of k_L calculated by Eq. (5) with U_G using the H_T in ELBC and the liquid viscosity and C_S in three columns as parameters, respectively. It is found in the figures that the k_L values in any systems and columns slightly increase with increasing U_G or are almost constant independent of U_G considering a small but complicated fluctuation of k_L with a wide range of change in U_G . It is also seen that k_L decreases with increasing liquid viscosity at a fixed value of U_G in any column and is little affected not only by the type of column and the H_T in the ELBC at a fixed liquid viscosity, but also by C_S except the case of $C_S = 0.05 \text{ kg/dm}^3$ in the NBC probably having a more complicated three phase flow. Furthermore, the k_L values observed in $0.5 \text{ kmol/m}^3 \text{ Na}_2\text{SO}_3$ solution without either CMC or C_S are shown to agree well with the literature values³ in the ELBC and NBC although a small difference in the U_G dependency of k_L between them. Based on a model of mass transfer into the surface of a turbulent liquid,^{13,14} the k_L value is shown to increase with $U_G^{1/4}$. Therefore, it is reasonable to conclude that the observed k_L values slightly increase with increasing U_G .

Dependence of k_L on d_B

Fig. 7 shows a plot of the obtained k_L values as a function of the obtained d_B values for the three types of bubble columns. It is seen in the figure that there are no clear dependence of k_L on d_B in any column although the k_L value clearly decreases with increasing liquid viscosity and almost independent of the type of column, H_T in the ELBC and C_S at a fixed value of d_B . The k_L values in the solution without either CMC or C_S are also found to be almost the same as those calculated from the correlations proposed by Calderbank and Moo-Yang (1961)¹⁵ and Akita and Yoshida (1974).¹⁶ and the data reported by Talvy et al.¹⁴ This suggests that the k_L determination employed are reasonable and useful.

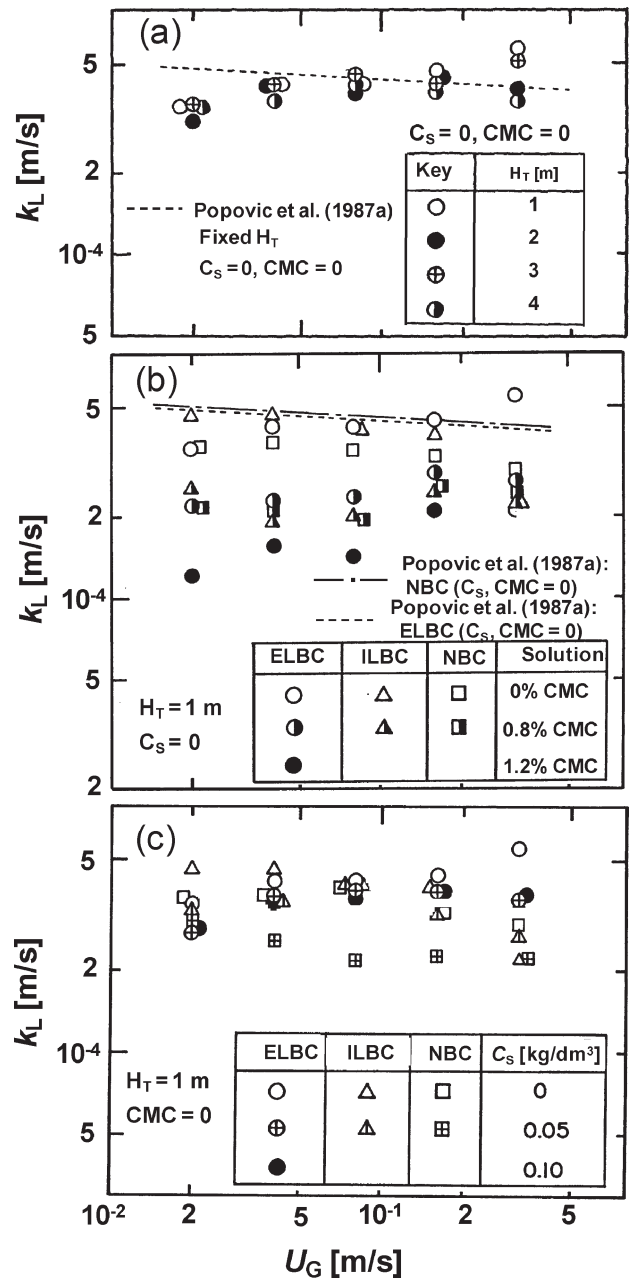


Fig. 6 – Effects of (a) H_T , (b) liquid viscosity and (c) C_S on k_L as a function of U_G

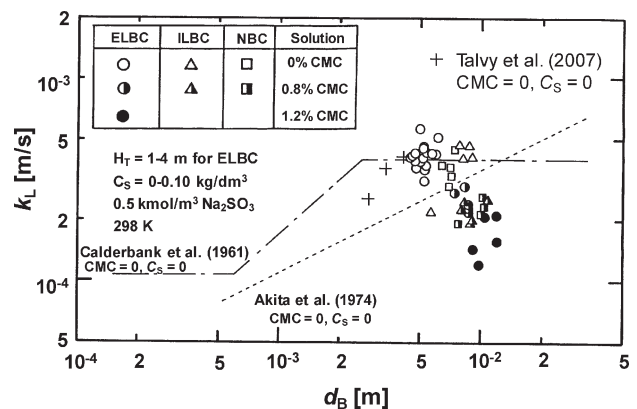


Fig. 7 – Dependence of k_L on d_B

Correlation of a with ϵ_G

The parallel relationships between a and ϵ_G as shown in Figs. 2, 3 and 4 lead to the plot of a as a function of ϵ_G . Fig. 8 shows such a plot for the data obtained in the three columns with aqueous sulfite solutions containing CMC at different concentrations. All the plots of a versus ϵ_G are seen to have the same slope of unity. Thus the values of a/ϵ_G obtained from Fig. 8 are plotted against the peculiar viscosity μ_p as shown in Fig. 9. Based on the figure, the correlation equations for a were obtained as Eq. (11) for ELBC and Eq. (12) for ILBC and NBC as shown in Table 3. Fig. 10 shows a comparison of the a values observed in this work with those calculated from the correlations Eqs. (11) and (12) and the literature correlation.³ The present correlations Eqs (11) and (12) are found to reproduce the observed a values within an accuracy of $\pm 20\%$. The literature correlation well agrees with the observed a values in the range of U_G lower than 0.1 m/s and overestimate the values increasingly with increase in U_G higher than 0.1 m/s. This is partly because their ELBC column design made a part of the bubbles recirculate through the downcomer into the riser giving the larger ϵ_G value in the whole column compared to the case of our ELBC.

The correlations of d_B for three columns were obtained by applying the correlations Eqs. (11) and (12) to Eq. (4). The results are shown in Table 3, being Eq. (13) for ELBC and Eq. (14) for ILBC and NBC. The correlations of k_L for any types of columns were derived by combining Eq. (9) with Eq. (11) for ELBC and Eq. (10) with Eq. (12) for ILBC and NBC through Eq. (5). The results are Eq. (15) for ELBC and Eq. (16) for ILBC and NBC as shown in Table 3. These correlations are very simple and useful to apply for estimating the values of a , k_L and hence $k_L a$ as well as d_B by knowing only both the ϵ_G value, predicted from Eqs. (6) and (7) for ELBC and Eq. (8) for ILBC and NBC, and the μ_p value measured simply by a Ostwalde-type viscometer. The viscometer should be calibrated with a Newtonian liquid of a known viscosity even in the case of a highly viscous liquid.

Conclusion

The results obtained in this work are summarized as follows.

(1) The a values in ELBC were only a little lower than those in ILBC and NBC in spite of the

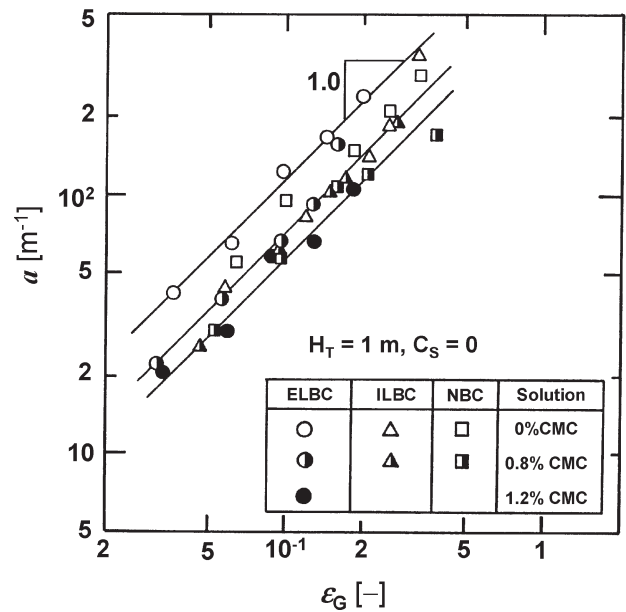


Fig. 8 – Correlation of a with ϵ_G

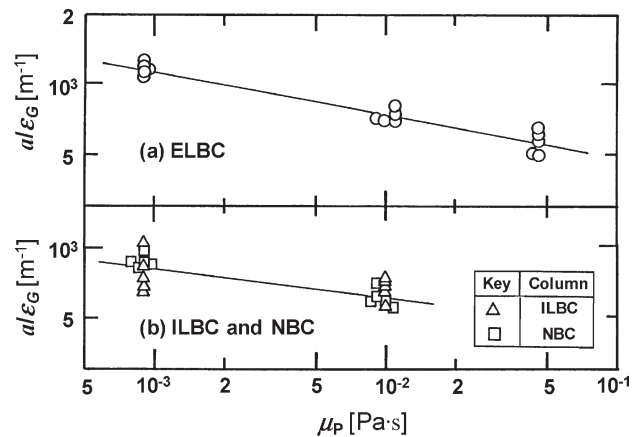


Fig. 9 – Dependence of a/ϵ_G on μ_p

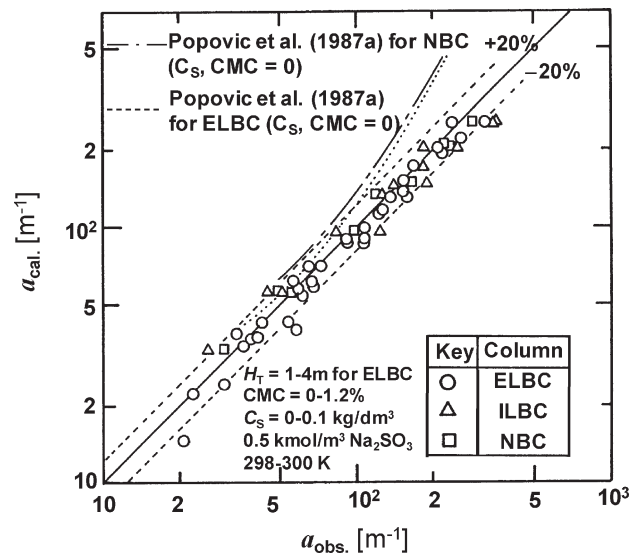


Fig. 10 – Comparison of observed a values with calculated ones from present and literature correlations

Table 3 – Correlations for a , d_B and k_L using μ_p

ELBC: $a = 320 \epsilon_G \mu_p^{-0.18}$ (11)	ILBC, $a = 323 \epsilon_G \mu_p^{-0.13}$ (12)
$d_B = 1.88 \times 10^{-2} \mu_p^{0.18}$ (13)	NBC: $d_B = 1.86 \times 10^{-2} \mu_p^{0.13}$ (14)
$k_L = 2.07 \times 10^{-4} \epsilon_G^{0.2} \mu_p^{-0.18}$ (15)	$k_L = 1.04 \times 10^{-4} \epsilon_G^{0.1} \mu_p^{-0.20}$ (16)

lower ε_G values in ELBC compared to those in ILBC and NBC. The a values in ILBC were almost equal to those in NBC.

(2) The a values in ELBC were independent of H_T in spite of the lower ε_G for the higher H_T . This is favorable for scale-up of ELBC. The a values in any type of columns decreased with increasing liquid viscosity and the d_B values correspondingly increased keeping the ε_G values little unaffected by the viscosity. The a values in any type of columns were also unaffected by C_S since the ε_G and d_B values were little influenced by it.

(3) The k_L values in three types of columns decreased with increasing liquid viscosity and were almost independent of C_S . The d_B and k_L values in any types of columns were almost independent of U_G and those in ELBC also of H_T . The data on k_L and d_B obtained in three types of columns satisfied a well-known relationship between k_L and d_B .

(4) The simple correlation equations for a , d_B and k_L for three types of columns were obtained as a function of ε_G and μ_P using the previous correlations for ε_G and $k_L a$ which were applicable to both two and three phase flows in the corresponding type of columns.

Nomenclature

A_d	– cross sectional area of downcomer, m^2
A_r	– cross sectional area of riser, m^2
a	– gas-liquid interfacial area, $1/m$
C_{oi}	– dissolved oxygen concentration at gas-liquid interface, $kmol/m^3$
C_{CaSO_4}	– cobalt sulfate (catalyst) concentration, $kmol/m^3$
C_S	– solid particle concentration based on bubble free volume, kg/m^3
D_d	– diameter of downcomer, m
D_i	– diameter of draft tube, m
D_{O_2}	– liquid diffusivity of oxygen, m^2/s
D_r	– diameter of riser, m
D_T	– diameter of ILBC and NBC, m
d_B	– average bubble diameter, m
d_p	– mean diameter of solid particles, m
H	– Henry's law constant, $kmol/Pa \cdot m^3$
H_T	– static liquid height above gas distributor, m
H_i	– height of draft tube, m
K	– fluid consistency index, $Pa \cdot s^n$
k_2	– second order rate constant, $m^3/kmol \cdot s$
k_L	– liquid phase oxygen transfer coefficient, m/s
$k_L a$	– volumetric gas-liquid oxygen transfer coefficient based on dispersion volume, $1/s$
n	– flow behavior index
P_{O_2}	– oxygen partial pressure, Pa
\bar{P}_{O_2}	– average oxygen partial pressure, Pa
R	– gas constant ($= 8.314$), $Pa \cdot m^3/kmol \cdot K$
R_{O_2}	– chemical oxygen absorption rate based on gas-sparged liquid volume, $kmol/m^3 \cdot s$
$R_{O_2}^{app}$	– chemical oxygen absorption rate based on total liquid volume in ELBC, $kmol/m^3 \cdot s$

T – temperature, K

U_G – superficial gas velocity, m/s

U_L – superficial liquid velocity in riser, m/s

V_L – total liquid volume in ELBC, m^3

$V_{L,r}$ – riser liquid volume, m^3

Greek letters

ε_G – gas holdup

ε_S – solid holdup ($= (1 - \varepsilon_G) C_S/\rho_S$)

μ_P – peculiar viscosity measured by Ostwalde-type viscometer, $Pa \cdot s$

ρ_S – density of solid particle, kg/m^3

Subscripts

cal – calculated value

obs – observed value

List of abbreviations

CMC – carboxymethyl cellulose

ELBC – external loop airlift bubble column

ILBC – internal loop airlift bubble column

IR – ion exchange resin

NBC – normal bubble column

References

1. Chisti, M. Y., "Airlift bioreactors" Elsevier Applied Science, New York, NY (1989)
2. Nakao, K., Suenaga, S., Takeda, K., Kimura, M., Robinson, C. W., "Mass Transfer in a Bubble Column with External Liquid Circulation" Preprints of 1st German-Japanese Symp. Bubble Columns, Schwerte, Germany, June 13-15, 1988, p.153-158.
3. Popovic, M., Robinson, C. W., Chem. Eng. Sci. **42** (1987a) 2811.
4. Popovic, M., Robinson, C. W., Chem. Eng. Sci. **42** (1987b) 2825.
5. Douek, R. S., Livingston, A. G., Johansson, A. C., Hewitt, G. F., Chem. Eng. Sci. **49** (1994) 3719.
6. Merchuk, J. C., Can. J. Chem. Eng. **81** (2003) 324.
7. Nakao, K., Azakami, F., Furumoto, K., Yoshimoto, M., Fukunaga, K., Can. J. Chem. Eng. **81** (2003) 444.
8. Freitas, C., Fialova, M., Zahradnik, J., Teixeira, J. A., Chem. Eng. Sci. **54** (1999) 5253.
9. Nakao, K., Harada, T., Furumoto, K., Kiefner, A., Popovic, M., Can. J. Chem. Eng. **77** (1999) 816.
10. Nakao, K., Suenaga, S., Furumoto, K., Yoshimoto, M., Fuunaga, K., Proceedings of The 9th Asian Conference on Fluidized-Bed and Three-Phase Reactors, "Circulating Liquid Velocity, Gas Holdup and Volumetric Gas-Liquid Mass Transfer Coefficient in a Three-Phase External Loop Airlift Bubble Column" Pacific Green Bay, Wanli, Taiwan, November 21-24, 2004, 313-318.
11. Reith, T., Beek, W. J., Chem. Eng. Sci. **28** (1973) 1331.
12. Schumpe, A., Deckwer, W.-D., Ind. Eng. Chem. Process Des. Dev. **21** (1982) 706.
13. Lamont, J. C., Scott, D. S., AIChE J. **16** (1970) 513.
14. Talvy, S., Cockx, A., Line, A., AIChE J. **53** (2007) 316.
15. Calderbank, P. H., Moo-Young, M. B., Chem. Eng. Sci. **16** (1961) 39.
16. Akita, K., Yoshida, F., Ind. Eng. Chem. Process Des. Dev. **13** (1974) 84.